

Assessing seizure dynamics by analysing the correlation structure of multichannel intracranial EEG

Kaspar Schindler,¹ Howan Leung,¹ Christian E. Elger¹ and Klaus Lehnertz^{1,2}

¹Klinik für Epileptologie and ²Helmholtz-Institut für Strahlen- und Kernphysik, University of Bonn, Bonn, Germany

Correspondence to: Kaspar Schindler, Klinik für Epileptologie, Sigmund-Freud-Strasse 25, 53105 Bonn, Germany

E-mail: kschindler@smile.ch

Epileptic seizures are commonly characterized as ‘hypersynchronous states’. This habit is doubly misleading, because seizures are not necessarily synchronous and are not unchanging ‘states’ but dynamic processes. Here the temporal evolution of the correlation structure in the course of 100 focal onset seizures of 60 patients recorded by intracranial multichannel EEG was assessed. To this end a multivariate method was applied that at its core consists of computing the eigenvalue spectrum of the zero-lag correlation matrix of a short sliding window. Our results show that there are clearly observable and statistically significant changes of the correlation structure of focal onset seizures. Specifically, these changes indicate that the zero-lag correlation of multi-channel EEG either remains approximately unchanged or—especially in the case of secondary generalization—decreases during the first half of the seizures. Then correlation gradually increases again before the seizures terminate. This development was qualitatively independent of the anatomical location of the seizure onset zone and therefore seems to be a generic property of focal onset seizures. We suggest that the decorrelation of EEG activity is due to the different propagation times of locally synchronous ictal discharges from the seizure onset zone to other brain areas. Furthermore we speculate that the increase of correlation during the second half of the seizures may be causally related to seizure termination.

Keywords: correlation structure; eigenvalue spectrum; intracranial EEG; multivariate time series analysis; seizure termination

Received May 17, 2006. Revised August 10, 2006. Accepted September 29, 2006. Advance Access publication November 1, 2006.

Introduction

In this study seizure dynamics is defined as the spatio-temporal evolution of electrical ictal activity as measured by intracranial EEG. Investigating seizure dynamics is highly important, because it may help to answer some of the most fundamental and yet debatable questions in epileptology like how the propagating ictal discharges affect the ongoing electrical activity of the brain or why seizures terminate. Answering these questions would lead to a deeper understanding of the collective action of large neuronal assemblies and potentially help to advance protocols for closed-loop brain stimulation in epilepsy patients (Osorio *et al.*, 2005; Morrell, 2006) or to improve therapies of life-threatening conditions like status epilepticus (Logroscino *et al.*, 2005). A typical evolution of intracranially recorded ictal EEG of focal onset seizures as assessed by standard visual analysis consists of initially low-voltage fast activity in a few channels, propagating to neighbouring channels and concurrently

slowing down and gaining amplitude. Seizure termination is then often heralded by bursts, i.e. groups of high-amplitude polyspike and slow waves separated by intervals of depressed activity. This typical evolution of ictal EEG from high to low dominant frequencies has been quantitatively corroborated by spectrographic analysis (Schiff *et al.*, 2000). However, the aim of applying mathematical methods to EEG analysis is not restricted to confirming the results of standard visual analysis. On the contrary, signal analysis techniques may transform ictal EEG signals in a way that structures hidden to clinical EEG reading are revealed. Ideally, these structures are amenable to quantitative analysis, further increasing the precision of the characterization of seizure dynamics. Though such an approach is essentially descriptive in the first instance, it may be the basis for better founded hypotheses about the causal mechanisms of seizure propagation and ending that are experimentally testable and

thereby help to answer the fundamental questions mentioned above.

In the past, seizure dynamics were investigated using many different mathematical methods, both linear and non-linear. For example Pijn *et al.* (1991) computed the correlation dimension D_2 of EEG signals recorded from different sites of the limbic cortex of rats in the course of kindling-induced seizures. They found that seizure spreading was associated with EEG activity characterized by lower values of D_2 . Franaszczuk and Bergey (1999) proposed a measure based on the residual covariance matrix of a multi-channel autoregressive model of EEG activity and found increased synchronization during intracranially recorded seizures of three patients, persisting for >2 h into the post-ictal period. The same authors used time-frequency decompositions by the matching pursuit method (Mallat and Zhang, 1993) to divide EEG seizure patterns into four stages designated initiation, transitional rhythmic bursting, organized rhythmic bursting and intermittent bursting activity (Franaszczuk *et al.*, 1998). They showed in a subsequent study that the signal complexity of the EEG channel closest to seizure onset increased during seizures (Bergey and Franaszczuk, 2001). Furthermore, segmentation techniques have been used to divide ictal EEG recordings into relatively stable sections in order to allow grouping of seizures with an overall similar pattern (Wendling *et al.*, 1996; Wu and Gotman, 1998). Recently, Schiff *et al.* (2005) detected distinct initiation and termination dynamics in human extra- and intracranially recorded ictal EEG by way of multivariate linear discrimination analysis. The study of the correlation matrix that consists of the zero or time-lagged correlations of all possible pairs of channels of a EEG recording has been proposed as a powerful way to quantify the degree of underlying neuronal collectivity (Kwapień *et al.*, 2000). Based on such an approach some generic, i.e. subject-independent non-invasive EEG features were extracted (Seba, 2003).

The aim of our study was to analyse the dynamic evolution of intracranially recorded EEGs during seizures with focal onset. To this end we define seizure onsets and endings in an observer-independent and quantitative way and then apply a method recently proposed by Müller *et al.* (2005) that allows for analysing the spatio-temporal correlation structure in multi-channel EEG recordings in an efficient and compact way. We demonstrate that during focal onset seizures this correlation structure shows a typical evolution, indicating an increase of overall zero lag correlations before seizure termination. Interestingly, correlations are higher throughout seizures that do not secondarily generalize.

Material and methods

EEG recordings

EEG signals were recorded intracranially by either strip, grid or depth electrodes (all manufactured by AD-TECH, WI, USA). Using

a Stellate Harmonie recording system (Stellate, Montreal, Canada; amplifiers constructed by Schwarzer GmbH, München, Germany) EEG signals were sampled at 200 Hz, i.e. at a sampling interval $\Delta t = 5$ ms, band-pass filtered between 0.1–70 Hz and A/D converted at 16 bit resolution. For analysis only bipolar derivations between nearest neighbour electrode contacts were used, in the following denoted by $EEG_i(t)$, where i runs over all channels. Note that the terms ‘channel’ and ‘bipolar derivation’ are used synonymously here. For square grid electrodes only the bipolar derivations along one dimension (perpendicular to the attachment points of the connecting wires) were used.

Defining seizure onsets and endings

To define seizures in an objective and therefore reproducible way and not just by subjective visual inspection of the EEG, we used the method illustrated in Fig. 1. First the absolute slope $S_i(t) = |\frac{\Delta EEG_i(t)}{\Delta t}|$ was computed, where i runs over all channels. $S_i(t)$ is an appropriate characteristic of epileptiform EEG, because it increases for both high-amplitude slow, but also low-amplitude fast activities (Schindler *et al.*, 2001) as are typically observed at the onset and during intracranially recorded seizures. In a second step, $S_i(t)$ was normalized to $\tilde{S}_i(t) = S_i(t)/\sigma_i^{\text{ref}}$, where σ_i^{ref} denotes the standard deviation of $S_i(t)$ during a reference period of 30 s length starting 2.5 s after the beginning of the EEG file containing the seizure. Finally, $\tilde{S}_i(t)$ was smoothed by a lagging moving average of 5 s duration. In Fig. 1A $\tilde{S}_i(t)$ is displayed for a seizure recorded with 37 intracranial channels. For each $EEG_i(t)$ presence of epileptiform activity was then empirically defined as $\tilde{S}_i(t) > 2.5$. Time of seizure onset T_{start} was determined when the number of channels $N_{\text{epi}}(t)$ recording epileptiform activity was at least three. Time of seizure ending T_{end} was defined as the moment when $N_{\text{epi}}(t)$ decreased <10% of its maximal value $N_{\text{epi}}^{\text{max}}$. Thus, for extensively propagating seizures the threshold in terms of channels recording epileptiform activity $N_{\text{epi}}^{\text{end}}$ was larger than the fixed threshold $N_{\text{epi}}^{\text{start}} = 3$ used to define seizure onset. By this definition of $N_{\text{epi}}^{\text{end}}$ a delayed detection of seizure ending due to postictal high-amplitude slowing or few isolated bursts of epileptiform activity could be prevented.

Analysis of multi-channel EEG correlation

If one tried to assess the correlation structure of n EEG channels by the running values of their pairwise correlations, one would have to work with $n(n-1)/2$ combinations. With the dozens of intracranial EEG channels studied here, this would yield hundreds to thousands of possible combinations. Given this huge amount of information, an analysis method that focuses on the essential correlation structure is therefore highly desirable. Such a method has recently been suggested by Müller *et al.* (2005) and allows for a very compact assessment of the evolving correlation structure in a computationally efficient way. The basic steps of this method are illustrated in Fig. 2. A sliding window w was moved along the EEG by small shifts of length t_{shift} . For each time point t_w , denoting the beginning of w , the EEG signals inside w were normalized channel-wise to $\tilde{EEG}_i(t)$ having zero mean and unit variance. Note that at any time the EEG signal recorded by m channels may be represented by a point in an m -dimensional vector space, a geometrical interpretation helpful to understand the meaning of eigenvectors introduced below. The normalized EEG signals were then used to compute the zero-lag (= equal time) correlation matrix C displayed in Fig. 2B. Each element of C corresponds to the zero-lag correlation coefficient defined

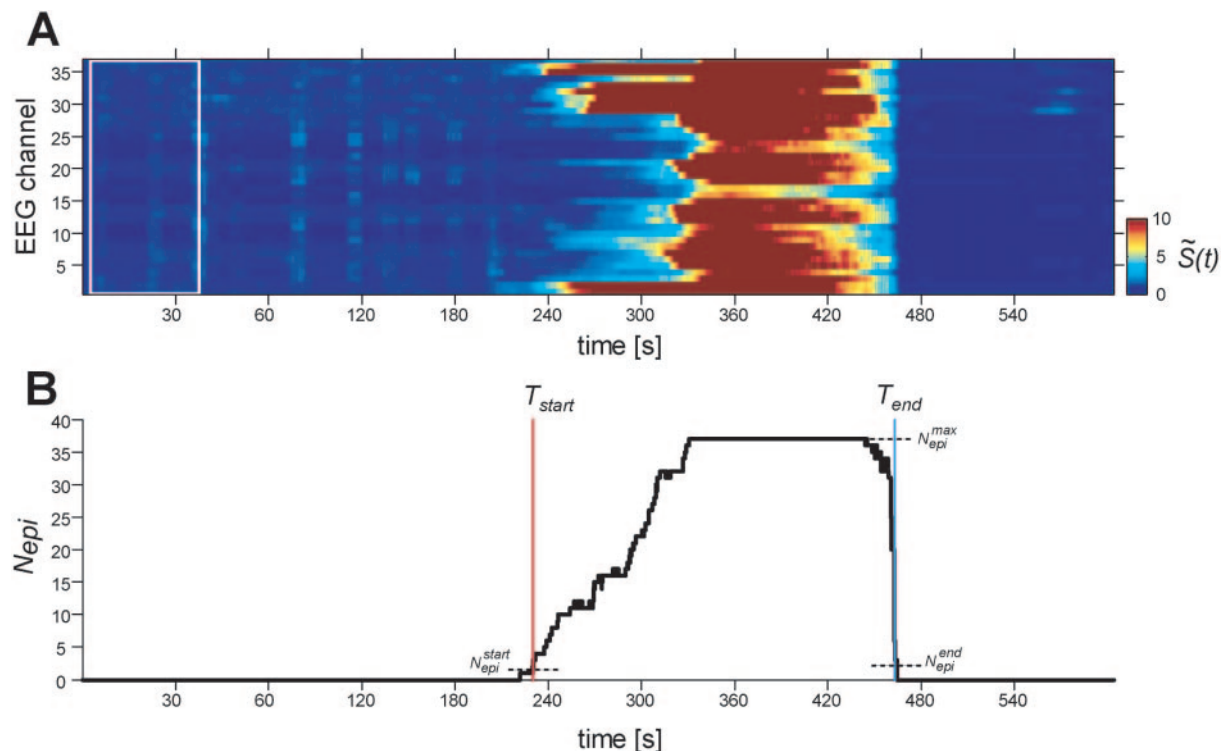


Fig. 1 Defining seizure onsets and endings. Shown is the analysis of a seizure with occipital lobe onset and secondary generalization recorded with 37 intracranial channels. The absolute slope $S_i(t)$ of the EEG from each channel i was divided by its standard deviation from a reference period of 30 s duration starting 2.5 s after the beginning of the data file containing the seizure (marked by the white rectangle). This yielded the normalized absolute slope $\tilde{S}_i(t)$, which was smoothed by a lagging moving average of 5 s duration and displayed in **A**. Epileptiform activity in a channel was empirically defined as $\tilde{S}_i(t) > 2.5$. The spatially non-contiguous appearance of epileptiform activity results from the display of channels, grouped by electrodes. The number of EEG channels detecting epileptiform activity $N_{\text{epi}}(t)$ is plotted in **B**. Time of seizure onset T_{start} (red line) is defined as $N_{\text{epi}}(t) \geq N_{\text{epi}}^{\text{start}} = 3$. Time of seizure end T_{end} (blue line) is defined as $N_{\text{epi}}(t) \leq 0.1 \cdot N_{\text{epi}}^{\text{max}}$. In the example shown the epileptiform activity propagated to all EEG channels and therefore $N_{\text{epi}}^{\text{max}} = 37$. Note the abrupt ending of epileptiform activity occurring almost simultaneously in all channels.

by: $C_{ij} = \frac{1}{w_l} \sum_{t \in w} \tilde{E}\tilde{E}G_i(t) \cdot \tilde{E}\tilde{E}G_j(t)$, where w_l denotes the length of the sliding window w . The correlation coefficient varies between +1 indicating perfect correlation and -1 if the two EEG signals are exactly anticorrelated. If $\tilde{E}\tilde{E}G_i(t)$ and $\tilde{E}\tilde{E}G_j(t)$ are completely uncorrelated then $C_{ij} = 0$. For all $i = j$, $C_{ij} = 1$, because each EEG signal is perfectly correlated with itself. From this, it directly follows that the sum of the elements of the main diagonal, which runs from the top left corner to the bottom right corner, called the trace of the matrix C , always equals the number of EEG signals. Furthermore, the correlation matrix C is symmetrical relative to its main diagonal, due to the commutative property of correlation, i.e. $C_{ij} = C_{ji}$. In the following we will use some fundamental results of the theory of linear algebra and specifically of the field of principal component analysis. A mathematically rigorous introduction to this subject is beyond the scope of this article and the interested reader is referred to standard texts such as the classic book by Jolliffe (2002). However, the analysis method may be qualitatively appreciated without the detailed mathematical background. The central point is that the distribution of the so-called eigenvalues λ of C is directly related to the correlation structure of the multi-channel EEG. The eigenvalues are computed by solving the equation $C\lambda_i = \lambda_i v_i$, where λ_i and v_i denote the eigenvalues and their associated eigenvectors. The eigenvectors form a new orthogonal basis of the m -dimensional vector space spanned by

the m EEG channels. Note that being orthogonal is synonymous to being uncorrelated. In the m -dimensional vector space spanned by the original EEG channels, the eigenvector v_{max} associated with the largest eigenvalue λ_{max} points in the direction of maximal average correlation. v_{max} is often referred to as the first principal component of a dataset. Given m orthogonal eigenvectors, C may then be diagonalized, that is linearly transformed into a matrix that only contains elements on its main diagonal. These elements turn out to be the eigenvalues λ and their amplitude is proportional to the amount of correlation in the direction of their associated eigenvectors. Because the sum of the diagonal elements of a matrix, i.e. its trace, remains unchanged under linear transformations, the sum of the eigenvalues λ must always equal m , which is the sum of the diagonal elements of the original correlation matrix C . Consequently, if some eigenvalues increase, at least one other eigenvalue has to decrease to keep the total sum of the eigenvalues constant. If the eigenvalues are sorted, e.g. in ascending order $\lambda_1 \leq \lambda_2 \leq \lambda_3 \dots \leq \lambda_{\text{max}}$, they form the so-called spectrum of the correlation matrix C . In Fig. 3 the two limiting cases for the shape of the eigenvalue spectrum are illustrated. Figure 3A shows an artificially created 'EEG' signal that is perfectly correlated. All entries of the correlation matrix C_{α} of this EEG signal are equal to 1, because each channel is perfectly correlated with any other (Fig. 3B) and the associated spectrum degenerates to a single

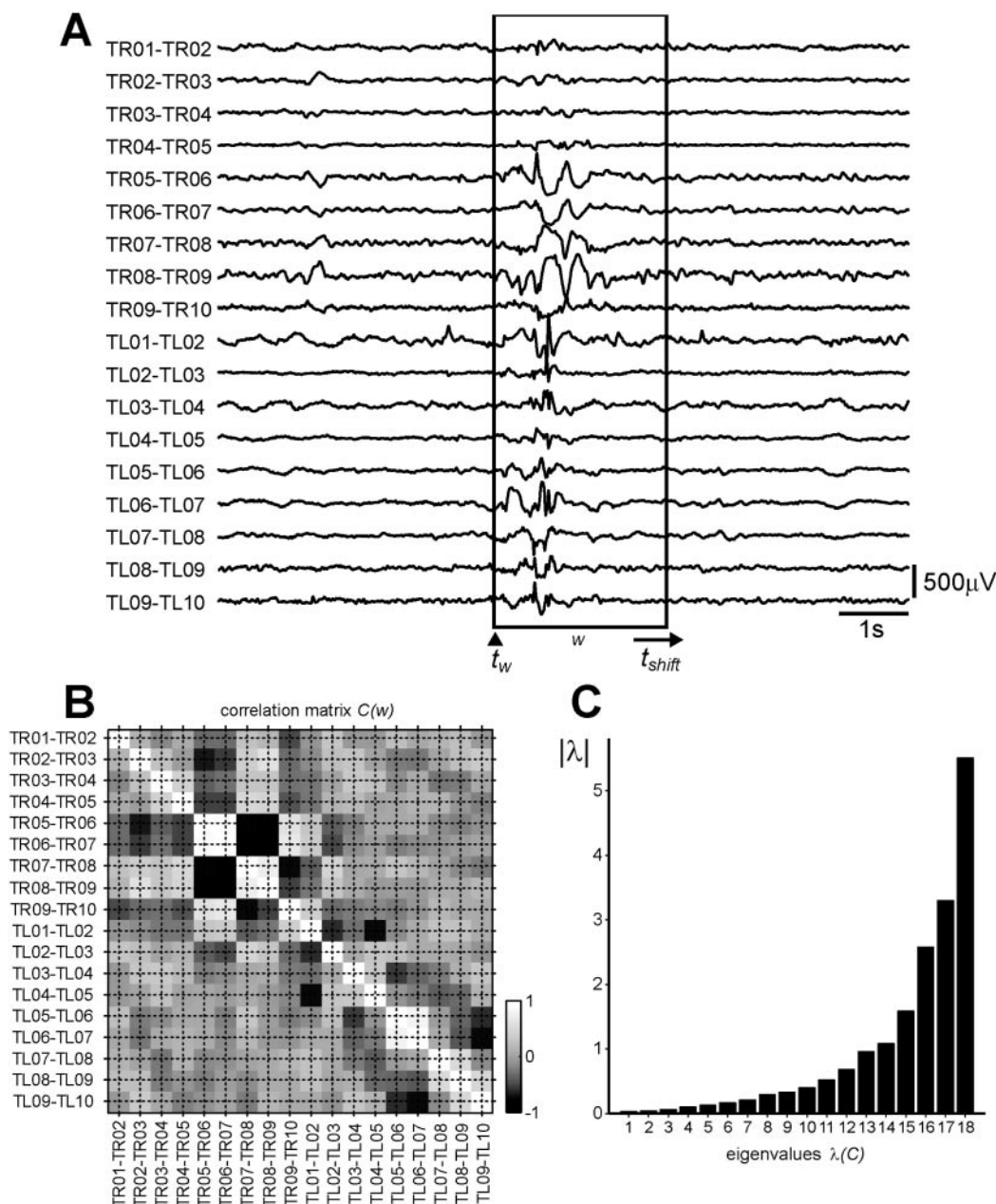


Fig. 2 Assessing the dynamics of EEG correlation structure proceeds in three steps. 1. The EEG channels inside a window w with a fixed length $w_1 = 2.5\text{s}$ are normalized to zero mean and unit variance (A). 2. The correlation matrix $C(w)$ is computed for the normalized EEG signals as displayed in B. Each element C_{ij} corresponds to the correlation coefficient between two normalized EEG signals and varies from -1 , when the two signals are perfectly anticorrelated, to $+1$, when they are perfectly correlated. Anticorrelation may for example be observed for the signal behaviour referred to as ‘negative phase reversals’ in clinical EEG reading as occurs between TR06-TR07 and TR07-TR08. The entries on the main diagonal $C_{i=i}$ running from the top left to the bottom right corner are equal to 1 , because each EEG signal is perfectly correlated with itself. $C(w)$ is symmetrical relative to the main diagonal, because correlation is commutative, that is $C_{ij} = C_{ji}$. For a symmetrical matrix like $C(w)$ with size $m \times m$ there are m eigenvalues $\lambda_{i=1:m}$, which fulfil the equation $C\lambda_i = \lambda_i v_i$, where v_i denotes the eigenvector belonging to the eigenvalue λ_i . 3. The eigenvalues are then sorted in ascending order, i.e. $\lambda_1 \leq \lambda_2 \leq \lambda_3 \dots \leq \lambda_{\text{max}}$ to form the spectrum of the correlation matrix C as displayed in C. Note the relatively large differences between the eigenvalues. The eigenvalue spectrum of $C(w)$ is then used as the column of a new matrix and associated with the time t_w of the first sampling point in w (see Fig. 4B). Then w is shifted by $t_{\text{shift}} = 0.005\text{ s}$, i.e. by one sampling point (200 Hz sampling rate), and the procedure is repeated.

eigenvalue λ_{max} (Fig. 3C). This may be understood by considering that in the vector space spanned by the 18 channels the points representing the ongoing EEG activity will fall on the straight line defined by $ch(1) = ch(2) = \dots = ch(18)$. The eigenvector v_{max}

will point exactly in the direction of this line, which is the only direction any correlation occurs for these ‘EEG’ data. In Fig. 3D the other limiting case is shown by an again artificially generated ‘EEG’. In this case each channel consists of random numbers and the

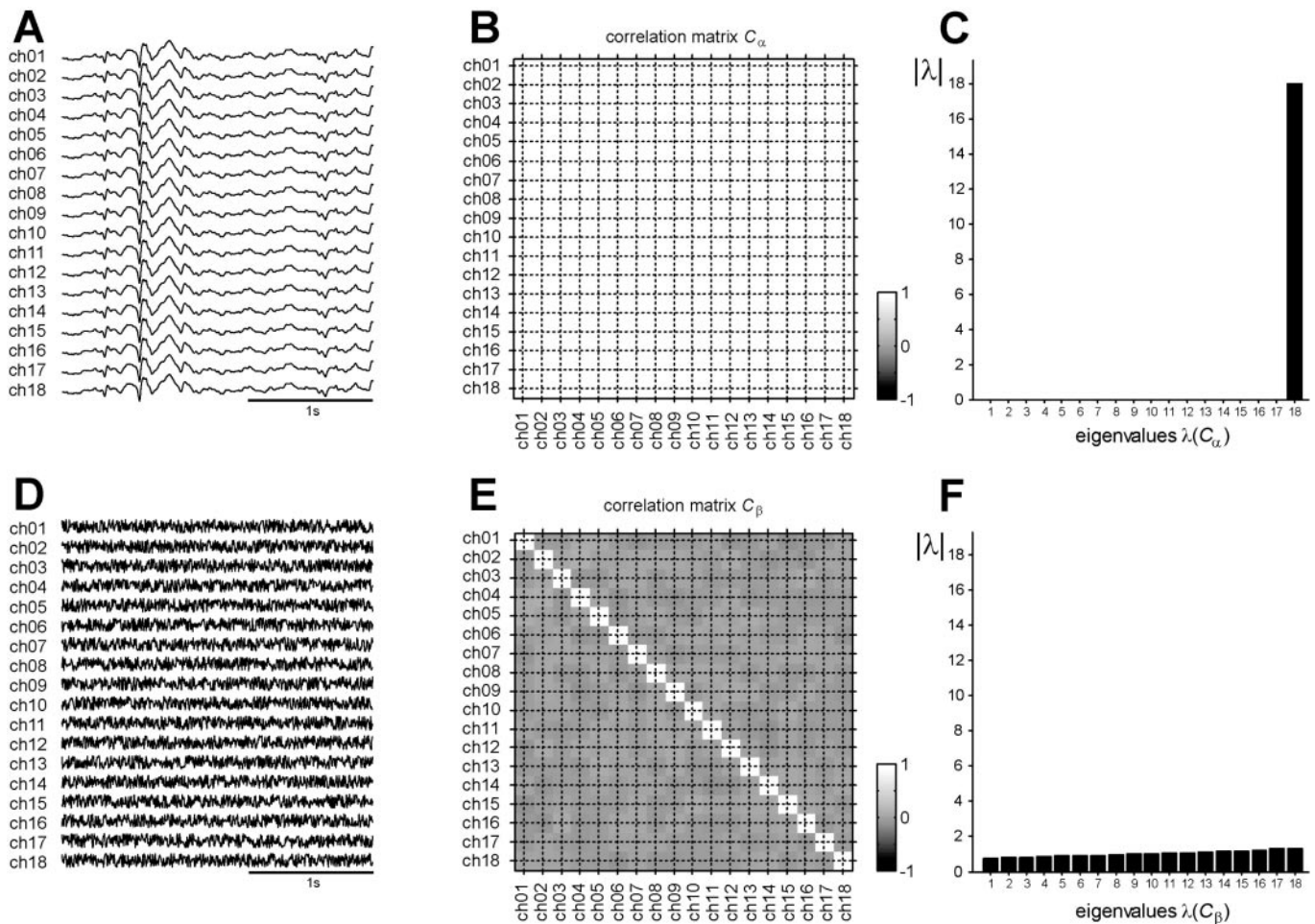


Fig. 3 Two limiting cases of correlation structure illustrated for artificially generated ‘EEG’ signals. In **A** a perfectly correlated multi-channel signal was created by using multiple copies of a single real EEG signal. The correlation matrix of this signal, denoted by C_α , has only elements equal to 1 and is plotted in **B**. The spectrum of C_α consists of a single eigenvalue of amplitude 18, i.e. the number of channels or the trace of C_α and is shown in **C**. The opposite case of an uncorrelated signal is the example plotted in **D**, with channels consisting of random numbers. The corresponding correlation matrix C_β has off-diagonal elements close to zero. Due to the finite length of the signal there occur random correlations and therefore the off-diagonal elements are not exactly zero. **(E)** The spectrum of C_β is almost flat and the eigenvalues are distributed around 1. The spectra of the real EEG signals will lie between the two distributions shown in **C** and **F**.

off-diagonal elements of the correlation matrix C_β are close to zero (Fig. 3E). They are not exactly zero, because due to the finite length of the data window there occur spurious random correlations. The corresponding spectrum of eigenvalues is almost flat with eigenvalues distributed around 1 (Fig. 3F). The points representing this random activity will approximate a so-called hypersphere (i.e. a sphere with dimension >3) in the 18-dimensional vector space, and the correlations in the directions of the different eigenvectors will be similar. For real EEG signals, the spectrum of the correlation matrix C will lie between these two extreme cases of perfectly correlated and almost completely uncorrelated activity. By successively sliding the window w along the multi-channel EEG, computing the spectrum of the correlation matrix $C(w)$ and then associating it with the time point t_w of the first sampling point of w the changing correlation structure of the EEG may be assessed. Although the largest amount of correlation is represented by λ_{\max} the rest of the spectrum also contains information about the changing correlations. Specifically, when the largest eigenvalue

decreases (increases) there may be a compensatory ‘broad-band’ increase (decrease) of many of the smaller eigenvalues, which may be easier to visualize. Therefore, we computed the complete spectrum and not just λ_{\max} . Note that even when the complete spectrum is computed there are only as many eigenvalues as EEG channels. This is the major advantage of the method applied here since it is truly multivariate, i.e. each eigenvalue reflects the correlations between all EEG channels, and thus allows for a very compact assessment of the evolving correlation structure. In the following, results are given as mean \pm standard deviation when possible.

Results

One hundred peri-ictal EEG recordings from 60 patients were retrospectively selected from the database of the Clinic of Epileptology of the University of Bonn. All the patients suffered from pharmacoresistant focal epilepsy and

underwent pre-surgical invasive evaluation because non-invasive studies had not been successful in localizing the seizure onset zones. All patients had signed informed consent that their clinical data might be used and published for research purposes.

On average 1.7 ± 0.6 seizures per patient (range: 1–4 seizures) were included. The average number of channels was 52 ± 21 (range 21–105), all recorded by intracranial strip, grid or hippocampal depth electrodes. Seizure onsets and endings had to be unequivocally definable by the method described above. According to this definition of seizure onset and ending the EEG files contained 124 ± 60 s of preictal and 210 ± 203 s of postictal time. Average seizure duration was 121 ± 81 s. There were 49 secondarily generalized and 51 complex partial seizures as judged by studying seizure semiology on the accompanying video. The average duration of secondarily generalized seizures was 123 ± 68 s, the average duration of complex partial seizures was 120 ± 90 s. Seizures were not selected based on anatomical location of seizure onsets or based on underlying pathology because we were interested in describing generic characteristics of the dynamics of focal onset seizures. They included 43 seizures with mesiotemporal, 27 with extramesial temporal, 21 with frontal, 7 with occipital and 2 with parietal lobe onset. This cohort is typical insofar as most patients with pharmacoresistant epilepsy who come to invasive EEG monitoring at our clinic suffer from temporal or frontal lobe epilepsy.

The length of the sliding window w was set to 500 sampling points, i.e. to a duration of 2.5 s. Longer and shorter durations of w from 100 to 1000 sampling points were tested but did not yield qualitatively different results. The sliding window w was advanced by one sampling point, i.e. $t_{\text{shift}} = 5$ ms before re-computing the eigenvalues of its correlation matrix $C(w)$ (Fig. 2C). The eigenvalues were then ordered according to ascending amplitudes and associated with the time point t_w of the first sampling point of w as the columns of a new matrix. Since the eigenvalues at the lower end of the spectrum were much smaller than λ_{max} (Fig. 2C), eigenvalues $\lambda_i(t)$ were separately normalized in time to $\tilde{\lambda}_i(t) = (\lambda_i(t) - \mu_{\text{ref}}^{\lambda_i}) / \sigma_{\text{ref}}^{\lambda_i}$ thereby improving their visualization. Here $\mu_{\text{ref}}^{\lambda_i}$ and $\sigma_{\text{ref}}^{\lambda_i}$ denote the mean and standard deviation of $\lambda_i(t)$ during a reference period of 30 s length starting 2.5 s after the beginning of the EEG file containing the seizure (i.e. the same reference period used to normalize the absolute EEG slope for defining seizure onsets and terminations). Figure 4 illustrates the results for the analysis of a complex partial seizure with extramesial temporal lobe onset recorded by 58 bipolar intracranial channels. The top panel (Fig. 4A) shows the time course of the number of channels detecting epileptiform activity $N_{\text{epi}}(t)$. Times of seizure onset and seizure ending are marked by the red and blue vertical lines respectively. In Fig. 4B the temporal evolution of the normalized eigenvalues $\tilde{\lambda}_i(t)$ was plotted. There is a clearly observable change of the correlation structure during the seizure. Approximately 10 s after T_{start}

the five to seven normalized eigenvalues at the upper end of the spectrum $[\tilde{\lambda}_{52-58}(t)]$ decrease, while there concurrently is a broad-band increase of eigenvalues $\tilde{\lambda}_{1-45}(t)$. This pattern corresponds to a ‘redistribution of the correlation structure’ to more dimensions of the vector space spanned by the eigenvectors of $C(w)$ and more eigenvalues are needed to explain a certain amount of correlation structure in the data. In other words, the EEG becomes decorrelated. As pointed out in the Material and methods section, a compensatory increase of some of the eigenvalues at the lower end of the spectrum is expected when the eigenvalues at the upper end decrease, because the sum of all eigenvalues has to remain constant and always be equal to the trace of the correlation matrix $C(w)$, which is 58 in the case shown. However, it is not predictable which of the eigenvalues will increase and therefore we computed the complete spectrum to better visualize the process of de- and recorrelation. In Fig. 4B the decorrelation begins to reverse around time 115 s and evolves as reflected by a steady decrease of the eigenvalues $\tilde{\lambda}_{1-45}(t)$ accompanied by an increase of the eigenvalues at the upper end of the spectrum well above the level at seizure start. This pattern reflects an increase of EEG correlation, which clearly begins before the seizure terminates. The original EEG signals are plotted from 5 s before T_{start} to T_{end} in Fig. 4C showing an electroencephalographic evolution typical for focal onset seizures beginning with low voltage fast activity, which spreads to other EEG channels and slowly transforms into rhythmic discharges of lower frequency but higher amplitudes. Note that contrary to the very obvious decorrelation pattern in Fig. 4B it is hardly possible to detect which parts of the original EEG signals are decorrelated by visual inspection. One of the reasons may be that visual attention automatically gets caught by larger amplitude signals like spikes, which seem to be highly correlated throughout the seizure, falsely supporting the impression of a ‘hypersynchronous state’. Figure 5 shows the temporal evolution of the normalized eigenvalues and three selected parts of the original EEG recording at higher temporal resolution to further illustrate how the changing ictal correlation structure is essentially hidden to standard visual analysis of the EEG. In Fig. 6A–C $\tilde{\lambda}_i(t)$ is shown for three secondarily generalized seizures of frontal lobe onset of the same patient recorded by 94 intracranial channels. In Fig. 6D–F the averages of the top six normalized eigenvalues $\tilde{\lambda}_{\text{mean}}^{89:94}(t)$ and of the 30 normalized eigenvalues from the lower end of the spectrum $\tilde{\lambda}_{\text{mean}}^{1:30}(t)$ were plotted. These graphs clearly illustrate the decrease of $\tilde{\lambda}_{\text{mean}}^{89:94}(t)$ compensated by the increase of $\tilde{\lambda}_{\text{mean}}^{1:30}(t)$, indicating increasing decorrelation during the first half of the seizures. Recorrelation starts again clearly before seizures terminate. Thus, the changes of $\tilde{\lambda}_i(t)$ were not only very similar for seizures of the same patient, but also showed qualitative similarity to the one displayed in Figs 4B and 5A though the seizures started in different lobes. By visual inspection of the temporal evolution of $\tilde{\lambda}_i(t)$ it appeared that for all seizures there was an increase of correlations before seizure

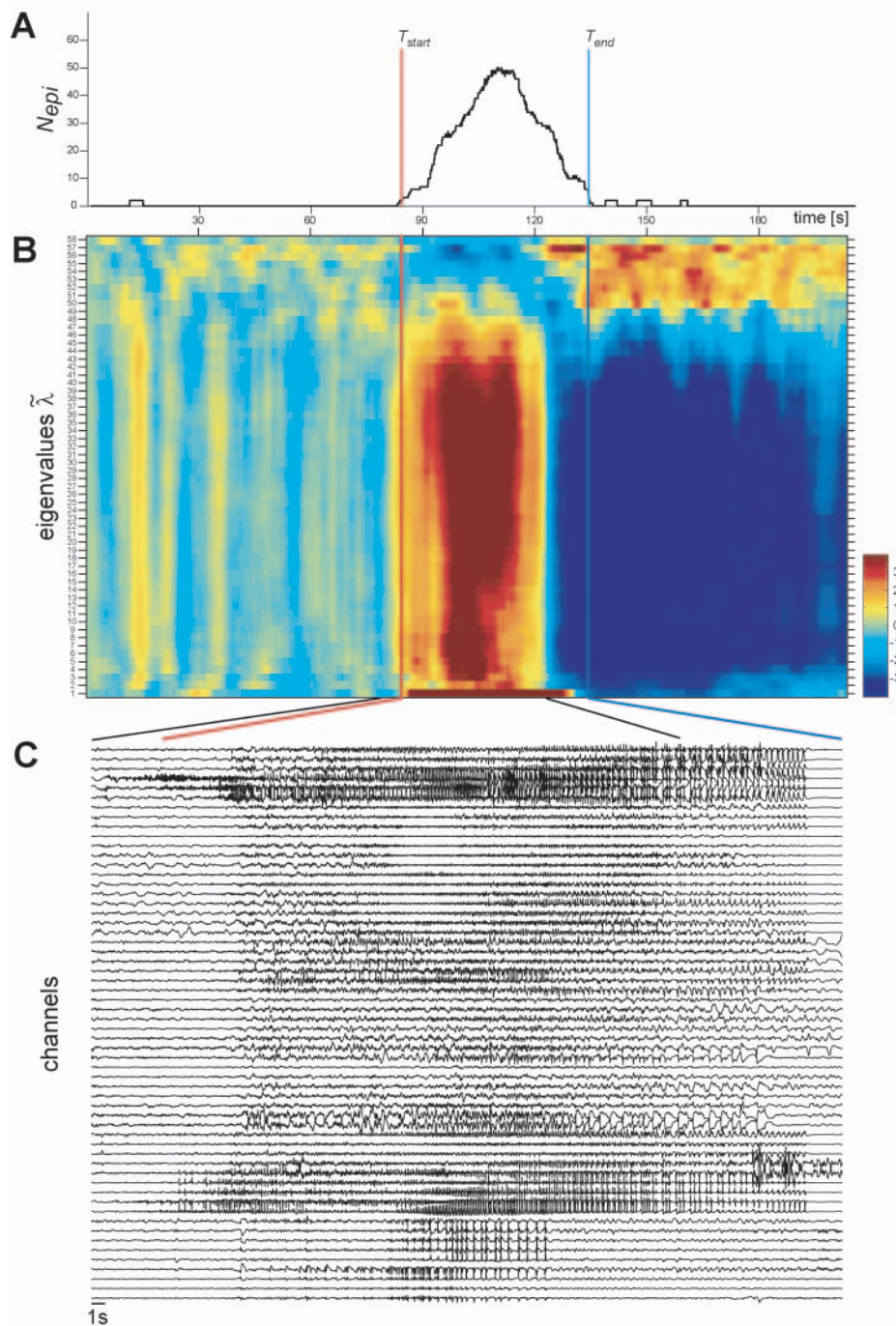


Fig. 4 Correlation analysis of complex partial seizure with temporal extramural onset. In **A** the amount of EEG channels recording epileptiform activity $N_{epi}(t)$ is plotted. Time of seizure onset T_{start} and of seizure ending T_{end} are marked by the red and blue vertical lines respectively. The results for computing the spectrum of the correlation matrix of a sliding window w are displayed in **B**, smoothed by a lagging moving average of 5 s duration. Each column corresponds to the spectrum of the correlation matrix computed when w reached this position in time, i.e. the spectrum was associated with the first sampling point included in w . Note that the lower end of the spectrum lies at the bottom of the graph, the upper end at the top. The eigenvalues $\lambda_i(t)$ were separately normalized in time to $\tilde{\lambda}_i(t) = (\lambda_i(t) - \mu_{ref}^{\lambda_i}) / \sigma_{ref}^{\lambda_i}$, where $\mu_{ref}^{\lambda_i}$ and $\sigma_{ref}^{\lambda_i}$ denote the mean and standard deviation of $\lambda_i(t)$ during a reference period of 30 s length starting 2.5 s after the beginning of the EEG file containing the seizure. By this normalization also the changes of the smaller eigenvalues at the lower end of the spectrum can easily be observed. Approximately 10 s after T_{start} the five to seven normalized eigenvalues, i.e. $\tilde{\lambda}_{52-58}(t)$, at the upper end of the spectrum decrease, while there is a broad-band increase of eigenvalues $\tilde{\lambda}_{1-45}(t)$, indicating that the EEG becomes decorrelated. Decorrelation begins to reverse around time 115 s and evolves with a steady decrease of eigenvalues $\tilde{\lambda}_{1-45}(t)$ accompanied by an increase of the eigenvalues at the upper end of the spectrum well above and below, respectively, the level at seizure start. This pattern reflects an increase of EEG correlation, which clearly begins before the seizure terminates. (**C**) The original EEG signals are plotted from 5 s before T_{start} to T_{end} . For a close-up see Fig. 5.

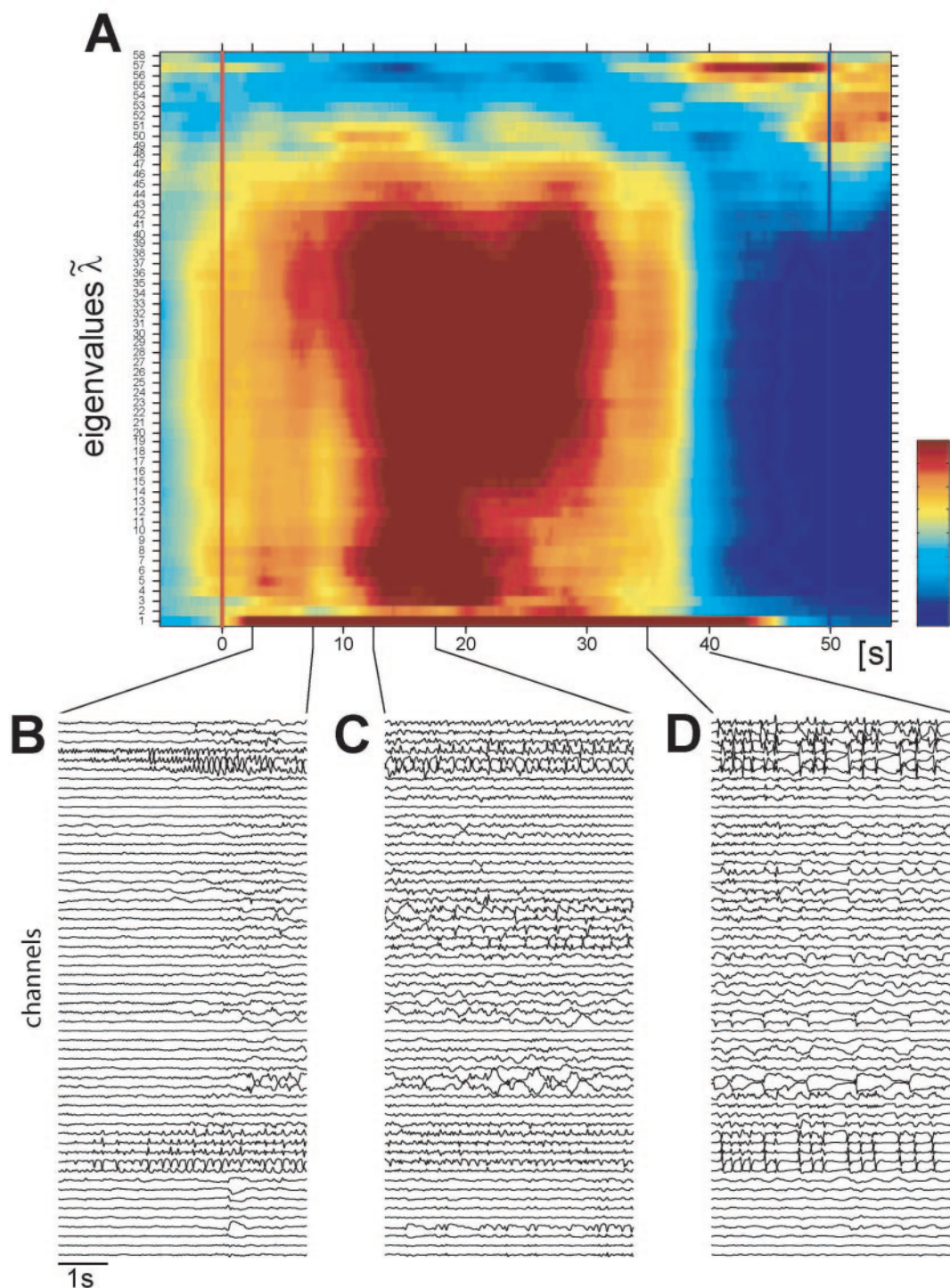


Fig. 5 Comparing changes of correlation structure and visual analysis of original EEG channels. **(A)** Close-up of the correlation structure of the complex partial seizure shown in Fig. 4. In panels **B–D** sections of the original EEG channels during periods with different correlation structures are displayed. Note that by visual analysis, the changes of the correlation structure, which are obvious in **A**, cannot be reliably detected. The vertical red and blue lines represent seizure onset and ending, respectively.

termination. To test whether this increase was dependent on the anatomical locations of seizure onsets we computed the mean of the five eigenvalues at the top end of the spectrum denoted by $\tilde{\lambda}_{\text{mean}}^{(\text{max}-4):\text{max}}$ and of the fifteen eigenvalues $\tilde{\lambda}_{\text{mean}}^{1:15}$

at the low end of the spectrum. Using a Wilcoxon rank sum test we then compared the temporal averages of $\tilde{\lambda}_{\text{mean}}^{(\text{max}-4):\text{max}}$ and of $\tilde{\lambda}_{\text{mean}}^{1:15}$ from a 2.5 s window beginning at seizure onset T_{start} and from a 2.5 s window ending at T_{end} (time of seizure

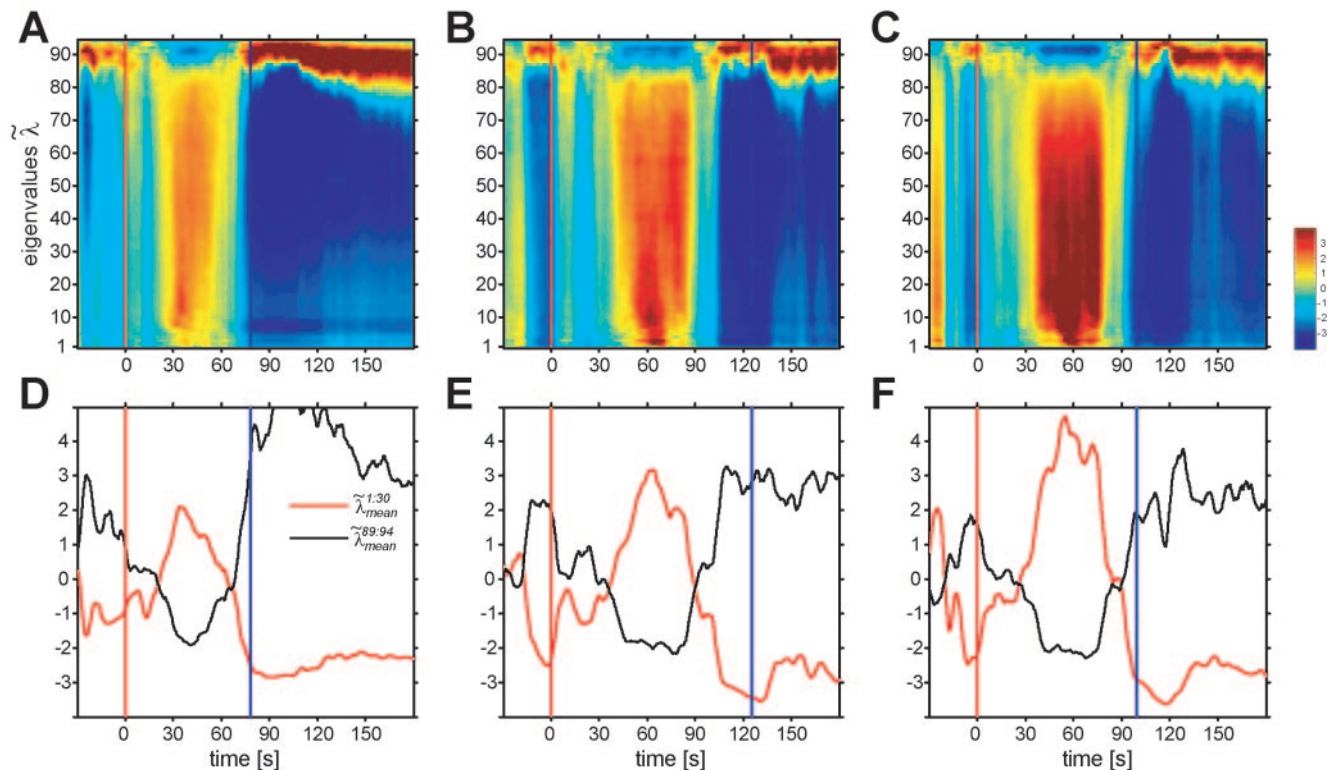


Fig. 6 The changes of the normalized eigenvalues $\tilde{\lambda}$ are very similar in seizures of the same patient, reflecting the stereotypical ictal evolution. The changing eigenvalue spectra of three secondarily generalized seizures with frontal lobe onset are displayed in **A–C**. In **D–F** the average of the six largest $\tilde{\lambda}_{\text{mean}}^{89:94}$ (black) and of the 30 smallest normalized eigenvalues $\tilde{\lambda}_{\text{mean}}^{1:30}$ (red) are shown. Note the strong increase of $\tilde{\lambda}_{\text{mean}}^{89:94}$, which is accompanied by a compensating decrease of $\tilde{\lambda}_{\text{mean}}^{1:30}$ during the first half of the seizure, indicating decorrelation of EEG activity. These time courses are then reversed, indicating an increase of correlation before the seizures terminate. The vertical red and blue lines represent seizure onsets and endings, respectively.

ending). This analysis was done separately for seizures with frontal lobe, mesiotemporal, and extramesial temporal lobe onsets and yielded statistically significant findings. The results shown in Fig. 7 clearly illustrate that the increase of correlation before seizure termination is qualitatively independent from the anatomical site of seizure onset and thus may be a generic property of focal onset seizures.

The decorrelation occurring during the first half of the seizures, reflected by a decrease of the eigenvalues at the top end of the spectrum and a compensating increase of the smaller eigenvalues, seemed to be more pronounced for the secondarily generalized seizures. To test this impression, we resampled all seizures to common duration. There was a decrease of $\tilde{\lambda}_{\text{mean}}^{(\text{max}-4):\text{max}}$ for secondarily generalized seizures lasting until normalized time 0.6 when $\tilde{\lambda}_{\text{mean}}^{(\text{max}-4):\text{max}}$ started to increase again (Fig. 8A). The time course of $\tilde{\lambda}_{\text{mean}}^{1:15}$ shows an opposite behaviour (Fig. 8D). For complex partial seizures $\tilde{\lambda}_{\text{mean}}^{(\text{max}-4):\text{max}}$ and $\tilde{\lambda}_{\text{mean}}^{1:15}$ stayed approximately unchanged until around normalized time 0.5 when they began to increase and decrease, respectively (Fig. 8B and E). In Fig. 8C and F $\tilde{\lambda}_{\text{mean}}^{(\text{max}-4):\text{max}}$ and $\tilde{\lambda}_{\text{mean}}^{1:15}$ computed for complex partial and for secondarily generalized seizures are plotted together. In this way it becomes obvious that during partial complex seizures the average correlation is higher

than in secondarily generalized seizures until approximately normalized time 0.9.

Finally, comparing the temporal means of $\tilde{\lambda}_{\text{mean}}^{(\text{max}-4):\text{max}}$ and $\tilde{\lambda}_{\text{mean}}^{1:15}$ from a 5 s window beginning in the middle (i.e. in the middle of the interval defined by T_{start} and T_{end}) of the non-resampled complex partial and secondarily generalized seizures proved them to be significantly different ($P < 0.005$, Wilcoxon rank sum test) as shown in Fig. 9.

Discussion

This study shows that there is a generic change of the correlation structure of focal onset seizures in humans. Specifically, this change indicates that the zero-lag correlation of multi-channel EEG either remains approximately unchanged or—especially in the case of secondary generalization—decreases during the first half of the seizures, but then gradually increases before the seizures terminate. We characterize this change of correlation structure as ‘generic’ because we observed it in all seizures independently of the anatomical location of the seizure onset zone or of seizure duration, number of channels, etc. In addition, our results corroborate that the time course of the eigenvalue spectrum of the zero-lag correlation matrix

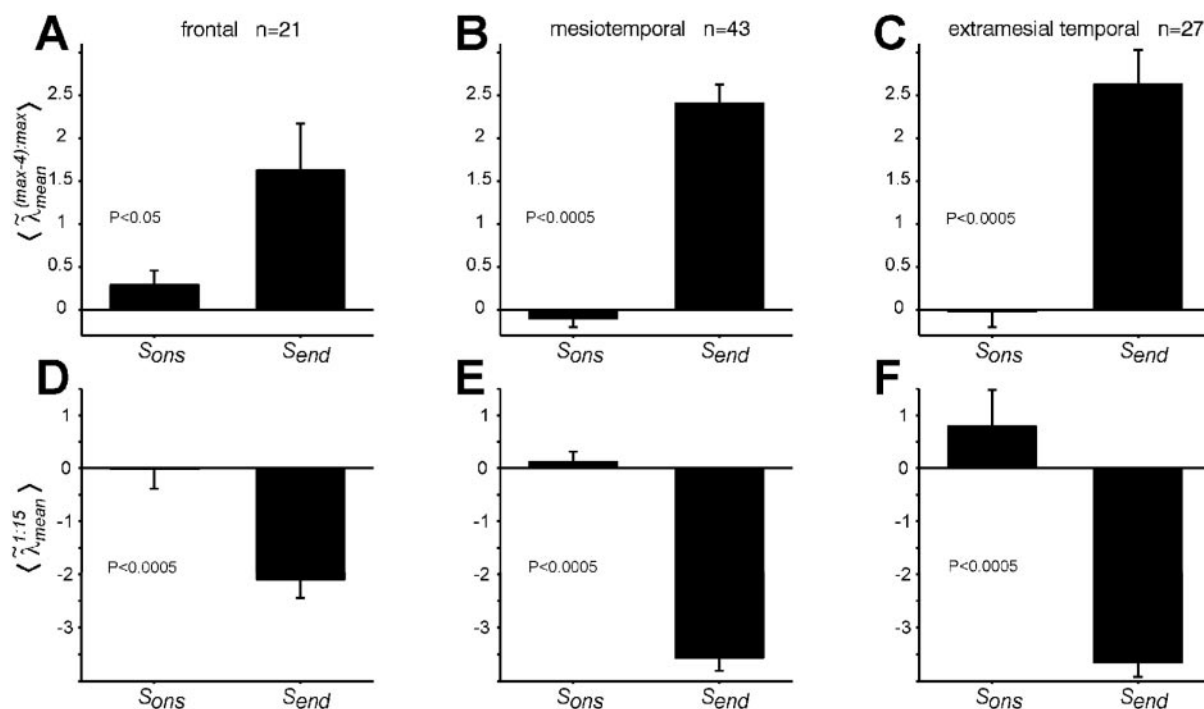


Fig. 7 Comparing correlations at seizure onset and before seizure termination. The temporal average of the mean of the five eigenvalues at the top end of the spectrum ($\langle \tilde{\lambda}_{\text{mean}}^{(\text{max}-4):\text{max}} \rangle$) from a 2.5 s window at seizure onset ($S_{\text{ons}} = [T_{\text{start}}, T_{\text{start}} + 2.5\text{s}]$) was compared to its temporal average from a window before seizure termination ($S_{\text{end}} = [T_{\text{end}} - 2.5\text{s}, T_{\text{end}}]$) for seizures with frontal lobe (A), mesiotemporal (B) and extramesial temporal (C) onsets by applying a Wilcoxon rank sum test. The corresponding results for the first 15 eigenvalues from the low end of the spectrum ($\langle \tilde{\lambda}_{\text{mean}}^{1:15} \rangle$) are displayed in D–F. Error bars indicate one standard error.

computed for a short sliding window is a powerful tool for EEG analysis. At present, the method is sensitive to linear correlations only and is not frequency dependent. Extensions of the method are currently underway to allow assessing possible non-linear correlations or correlations restricted to specific frequency bands.

‘Hypersynchrony’ revisited

Epileptic seizures are commonly characterized as ‘hypersynchronous’. This habit is confusing, because the term ‘hypersynchrony’ is used to describe both spatially extended electroencephalographic patterns and very localized neuronal discharges. On one hand high-voltage EEG signals with changes of amplitudes that are correlated across channels have been referred to as ‘hypersynchronous’. Examples are the EEG patterns of ‘hypnagogic hypersynchrony’ (Gibbs and Gibbs, 1950) consisting of paroxysmal large amplitude bursts of slow EEG waves in children during drowsiness, ‘hypersynchronous delta activity’ associated with somnambulism (Blatt *et al.*, 1991) or ‘hypersynchronous spike-and-waves’ of primary generalized epilepsies. On the other hand Penfield suggested that the focal collective firing of cortical neurons producing large amplitude EEG signals like epileptic spikes should be called ‘hypersynchrony’ (Penfield and Jasper, 1954). This ambiguity in the use of the term ‘hypersynchrony’ is growing more acute when studying the

dynamics of seizures with focal onset. The development of a ‘hypersynchronous’ EEG pattern with correlated amplitudes across multiple channels does not logically follow from the localized hypersynchrony of discharging neurons inside the seizure onset zone. On the contrary, due to the finite and different axonal conduction times, one might expect that the locally synchronous ictal discharges generated inside the seizure onset zone will propagate at different velocities and reach distant cortical areas with time delays relative to each other (Milton, 2003). Thereby the EEG correlation structure may be expected to change potentially even indicating a decrease of zero-lag correlation on a larger scale that includes seizure onset and seizure spreading zones. Thus we postulate that delays in propagation of locally synchronized epileptic potentials induce zero-lag decorrelation of the EEG activity during seizure spreading. Assuming that secondarily generalized seizures have more extensive spreading than complex partial seizures, this mechanism might also explain why the EEG decorrelation is stronger during the former. However, based on our data we cannot rule out that the causal relationship between spreading of ictal activity and decorrelation is opposite, i.e. that decorrelated neuronal activity is the reason why the ictal activity may propagate. Though this interpretation is supported by models of neuronal transient synchrony during propagation of activity through neural networks (Golomb, 1998), it leaves open the question what other mechanism would induce the

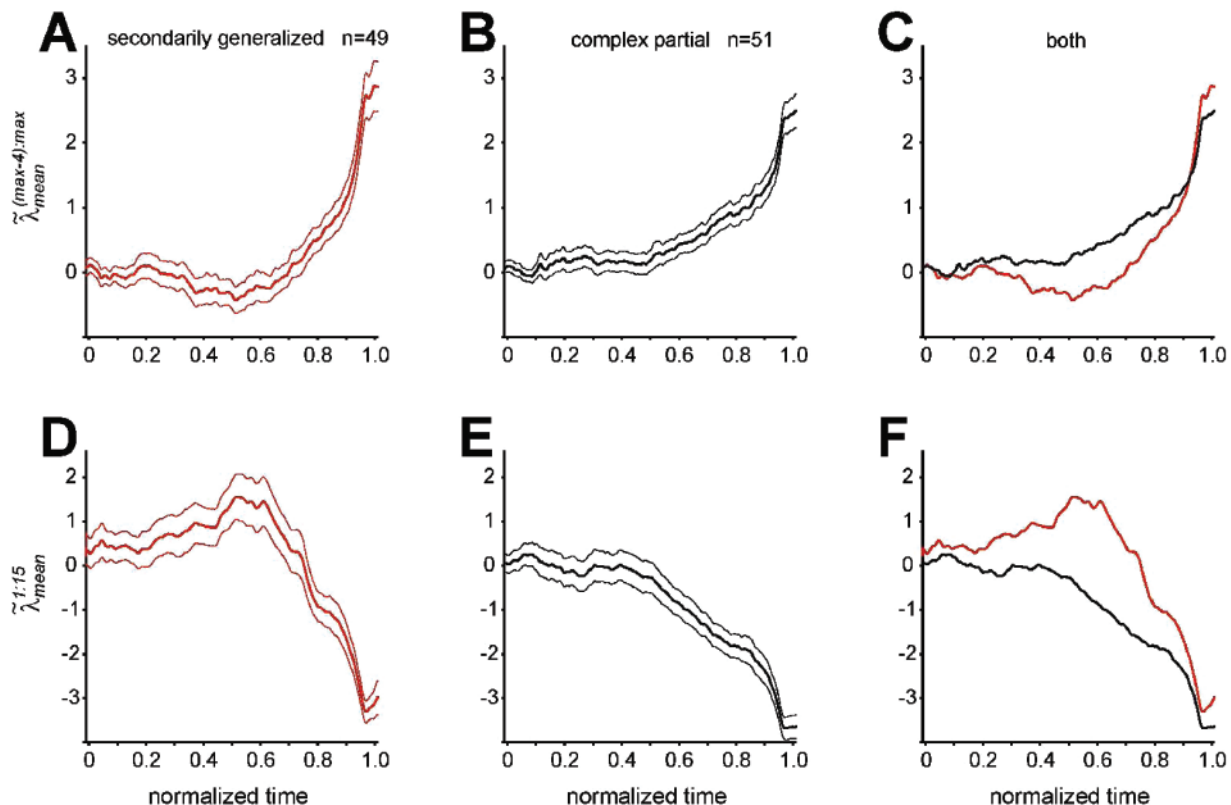


Fig. 8 Average change of correlation of complex partial and secondarily generalized seizures resampled to the same duration. (A) Time course of the average of the five largest normalized eigenvalues $\tilde{\lambda}_{mean}^{(max-4):max}$ (thick lines) and standard errors (thin lines) of all 49 secondarily generalized seizures. (B) $\tilde{\lambda}_{mean}^{(max-4):max}$ computed for the 51 complex partial seizures. In C the two averages are superimposed. Standard errors are not shown for better visibility. $\tilde{\lambda}_{mean}^{(max-4):max}$ for complex partial seizures (black) starts to increase before $\tilde{\lambda}_{mean}^{(max-4):max}$ for secondarily generalized seizures (red). D–F show the corresponding plots for the averages and standard errors of the 15 smallest normalized eigenvalues $\tilde{\lambda}_{mean}^{1:15}$. The decorrelation during secondarily generalized seizures is best reflected by the increase of $\tilde{\lambda}_{mean}^{1:15}$ until approximately normalized time 0.6.

decorrelation in the first place. Another possible interpretation combines the two previous ones and postulates a positive feed-back loop in the sense that the spreading ictal discharges induce decorrelated neuronal activity that further promotes the propagation of ictal discharges leading to a further increase of decorrelation, etc. Such a positive feed-back process might explain why many seizures showed first a gradual and then a more rapid or even ‘explosive’ spreading. For example during the seizure displayed in Fig. 4, the number of EEG channels recording epileptiform activity starts to increase much stronger shortly after time point 90 s. Though this interpretation also has to be considered with care, because observing decorrelated EEG signals does not necessarily imply decorrelated activity on a smaller spatial scale, it is interesting that desynchronized neuronal firing was recently observed in rat hippocampal slices during ‘seizure-like events’ (Netoff and Schiff, 2002). One way to experimentally test the hypothetical causal relationship between spreading of ictal activity and EEG decorrelation could be to electrically stimulate the seizure onset zone. In a first step, different stimulation parameters might be characterized by their de- or hypercorrelating effect as measured

for example by the method presented in this study and then tested for seizure abortion or prevention.

Our results, that ictal EEG activity of focal onset seizures may initially be rather decorrelated than ‘hypersynchronous’, is furthermore consistent with the findings of Wendling *et al.* (2003). These authors described significant spatial decorrelation during initial fast ictal discharges as recorded by EEG depth electrodes.

Why do seizures end?

Why seizures terminate is one of the most important, but still unanswered question of epileptology. We consistently found an increase of correlation before the seizures ended, reflected by an increase of the largest eigenvalues and a compensatory decrease of the smaller eigenvalues. Note that this increase of correlation started around 0.6 on the time scale normalized to seizure length shown in Fig. 8, i.e. clearly before seizure termination. Thus, it was certainly not an artefact of including postictal activity in the seizure period. This increase of correlation occurred for both partial-complex as well as secondarily generalized seizures.

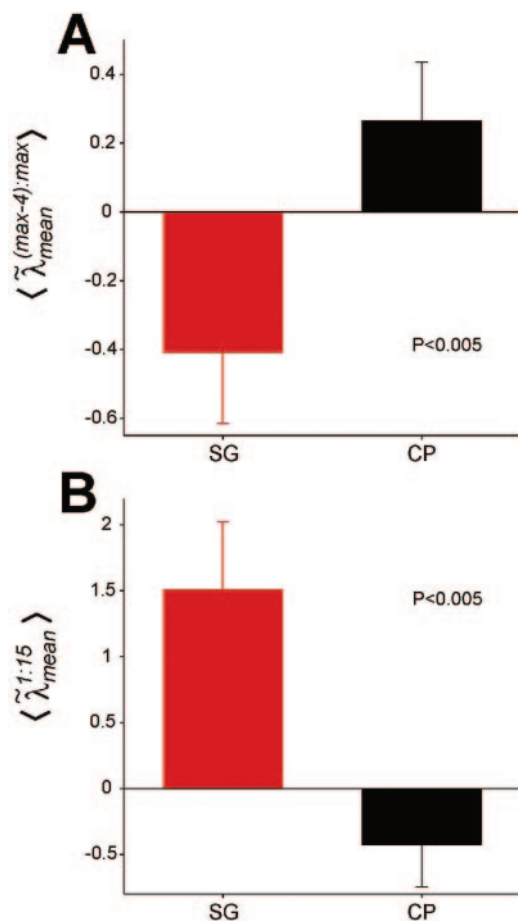


Fig. 9 (A) The temporal means of the average of the 5 eigenvalues at the top, $\langle \tilde{\lambda}_{\text{mean}}^{(\text{max}-4):\text{max}} \rangle$, and of the 15 eigenvalues at the low end of the spectrum, $\langle \tilde{\lambda}_{\text{mean}}^{1:15} \rangle$, from a 5 s window beginning in the middle (i.e. in the middle of the interval defined by T_{start} and T_{end}) of the 49 secondarily generalized (SG, red) and of the 51 complex partial (CP, black) seizures were significantly different ($P < 0.005$, Wilcoxon rank sum test) **(B)**. The significantly lower values of $\langle \tilde{\lambda}_{\text{mean}}^{(\text{max}-4):\text{max}} \rangle$ and larger values of $\langle \tilde{\lambda}_{\text{mean}}^{1:15} \rangle$ for secondarily generalized relative to complex partial seizures point to a stronger decorrelation of the former. Error bars indicate one standard error.

However, in the former it started earlier relative to seizure duration.

Importantly, our results are consistent with an extensive series of *in vivo* cat experiments including multi-site intracellular and extracellular as well as local cortical field potential recordings by which Steriade and colleagues investigated initiation, development and cessation of seizures (summarized in Timofeev and Steriade, 2004). In the initial stage of seizures they observed time-lags between cortical recordings of up to 150 ms, but the degree of synchrony progressively increased towards the late seizure stage (Topolnik *et al.*, 2003). When all the affected neuronal pools were drawn into highly synchronous paroxysmal activity, the seizures stopped. As one possible electrophysiological mechanism underlying seizure termination, the authors proposed that Na^+ - and Ca^{2+} -activated potassium

currents overcome hyperpolarization-activated depolarizing ionic currents. Presumably, activation of potassium currents is most effective in hyperpolarizing neuronal membranes and suppressing ictal activity when it occurs simultaneously in large neuronal networks. Therefore the increase of correlated EEG activity before seizure end could turn out to be an active seizure termination mechanism and not just an epiphenomenon of another underlying process. If an increase of collective neuronal activity as reflected by EEG correlation is necessary to stop ictal discharges, then this may also explain why seizures often stop almost simultaneously in many or all intracranial electrodes as may for example be seen in Fig. 1. Furthermore, a relatively delayed onset of increasing correlation might then lead to secondarily generalization as we observed in our study (Fig. 8C and F).

Our results are also consistent with the study by Schiff *et al.* (2005) who computed sums of arbitrary-lag and zero-lag cross correlations of 12 intracranially recorded ictal EEGs. They found a significant increase of the summed cross correlation at arbitrary lag only during the middle phase of seizures, which might be explained by the ictal discharges spreading from the seizure onset zone to other brain areas as postulated above. Furthermore, they also observed an increase of zero-lag cross correlations towards the end of the seizure, extending into the post-ictal period.

The relatively slow build up of correlation on a time scale of tens of seconds might be compatible with a non-synaptic mechanism of synchronization such as Ca^{2+} -mediated glutamate release from astrocytes or potassium diffusion through glial networks (Amzica *et al.*, 2002; Tian *et al.*, 2005). A synaptically mediated way of synchronization could be the involvement of cortico-thalamo-cortical loops (Neckelmann *et al.*, 1998; Meeren *et al.*, 2002; Salami *et al.*, 2003). In a recent study Guye *et al.* (2006) investigated thalamic activity during temporal lobe seizures in 13 patients and demonstrated increasing synchronization as assessed by non-linear correlation between temporal structures and the thalamus. The authors speculated whether thalamic involvement might be a mechanism for seizure spreading as has been suggested by the study of rat models of limbic epilepsy (Bertram *et al.*, 2001), but is not corroborated by the findings of Timofeev and Steriade (2004) who found minimal thalamic involvement during seizure development. Whatever importance of the thalamus in regard to seizure spreading may finally be revealed, the concept of cortico-thalamic interactions as a mechanism for seizure spreading does not preclude its potential role in seizure termination. Possibly a certain amount of seizure spreading is even necessary to set up the slow and synchronous cortical oscillations that then lead to simultaneous neuronal hyperpolarizations and ultimately to seizure termination.

There are a number of possible extensions and practical applications of the work presented here. In this study we explicitly wanted to characterize the dynamic evolution of electroencephalographic activity during seizures. Therefore, we had to select seizures with an objectively definable

beginning and end. However, there is often epileptiform activity that may not be clearly delimited and it might turn out that its correlation structure may be helpful in this regard. Also so-called 'subclinical' ictal activity may possibly be better detected by analysing the changes of the EEG correlation structure. Furthermore, there are short lasting broad-band increases of the smaller normalized eigenvalues before clinically manifest seizures as can be seen in Figs 4B and 6. It will be interesting to investigate whether the characteristics of these fluctuations show specific changes in the pre-seizure time period indicating an increased probability of seizure occurrence.

Another possible extension of the work presented here is to examine which brain regions are responsible for the changes of the EEG correlation structure, thereby possibly gaining new insights into the organization of epileptogenic neuronal networks. A related subject would be to measure time delays between ictal activities recorded from intracranial electrodes to verify the hypothesis that these delays are responsible for the observed decorrelation. Finally, the changes of the EEG correlation structure may turn out to be helpful for timing and measuring the effect of closed-loop brain stimulation for seizure abortion or prevention (Morrell, 2006).

Acknowledgements

K.S. was supported by a scholarship of the SSMBS (Schweizerische Stiftung für Medizinisch-Biologische Stipendien) donated by Roche. H.L. was supported by the Henry CH Leung Fellowships. C.E.E. and K.L. acknowledge support from the Deutsche Forschungsgemeinschaft (SFB TR3).

References

- Amzica F, Massimini M, Manfredi A. Spatial buffering during slow and paroxysmal sleep oscillations in cortical networks of glial cells in vivo. *J Neurosci* 2002; 22: 1042–53.
- Bergey GK, Franaszczuk PJ. Epileptic seizures are characterized by changing signal complexity. *Clin Neurophysiol* 2001; 112: 241–9.
- Bertram EH, Mangan PS, Zhang D, Scott CA, Williamson JM. The midline thalamus: alterations and a potential role in limbic epilepsy. *Epilepsia* 2001; 42: 967–78.
- Blatt I, Peled R, Gadoth N, Lavie P. The value of sleep recording in evaluating somnambulism in young adults. *Electroencephalogr Clin Neurophysiol* 1991; 78: 407–12.
- Franaszczuk PJ, Bergey GK. An autoregressive method for the measurement of synchronization of interictal and ictal EEG signals. *Biol Cybern* 1999; 81: 3–9.
- Franaszczuk PJ, Bergey GK, Durka PJ, Eisenberg HM. Time-frequency analysis using the matching pursuit algorithm applied to seizures originating from the mesial temporal lobe. *Electroencephalogr Clin Neurophysiol* 1998; 106: 513–21.
- Gibbs FA, Gibbs EL. Atlas of electroencephalography. Normal controls. Vol. 1. Cambridge, MA: Addison-Wesley; 1950.
- Golomb D. Models of neuronal transient synchrony during propagation of activity through neocortical circuitry. *J Neurophysiol* 1998; 79: 1–12.
- Guye M, Regis J, Tamura M, Wendling F, McGonigal A, Chauvel P, et al. The role of corticothalamic coupling in human temporal lobe epilepsy. *Brain* 2006; 129: 1917–28.
- Jolliffe IT. Principal component analysis, 2nd edn. New York: Springer Series in Statistics; 2002.
- Kwapień J, Drozd S, Ioannides AA. Temporal correlations versus noise in the correlation matrix formalism: an example of the brain auditory response. *Phys Rev E Stat Phys Plasmas Fluids Relat Interdiscip Topics* 2000; 62: 5557–64.
- Logroscino G, Hesdorffer DC, Cascino G, Hauser WA, Coeytaux A, Galobardes B, et al. Mortality after a first episode of status epilepticus in the United States and Europe. *Epilepsia* 2005; 46 (Suppl 11): 46–8.
- Mallat S, Zhang Z. Matching pursuits with time-frequency dictionaries. *IEEE Trans Signal Process* 1993; 41: 3397–415.
- Meeren HK, Pijn JP, Van Luijtelaar EL, Coenen AM, Lopes da Silva FH. Cortical focus drives widespread corticothalamic networks during spontaneous absence seizures in rats. *J Neurosci* 2002; 22: 1480–95.
- Milton J. Insights into seizure propagation from axonal conduction times. In: Milton J and Jung P, editors. *Epilepsy as a dynamic disease*. Berlin: Springer-Verlag; 2003. p. 15–23.
- Morrell M. Brain stimulation for epilepsy: can scheduled or responsive neurostimulation stop seizures? *Curr Opin Neurol* 2006; 19: 164–8.
- Müller M, Baier G, Galka A, Stephani U, Muhle H. Detection and characterization of changes of the correlation structure in multivariate time series. *Phys Rev E Stat Nonlin Soft Matter Phys* 2005; 71: 046116.
- Neckelmann D, Amzica F, Steriade M. Spike-wave complexes and fast components of cortically generated seizures III. Synchronizing mechanisms. *J Neurophysiol* 1998; 80: 1480–94.
- Netoff TL, Schiff SJ. Decreased neuronal synchronization during experimental seizures. *J Neurosci* 2002; 22: 7297–307.
- Orosio I, Frei MG, Sunderam S, Giftakis J, Bhavaraju NC, Schaffner SF, et al. Automated seizure abatement in humans using electrical stimulation. *Ann Neurol* 2005; 57: 258–68.
- Penfield W, Jasper H. Hypersynchrony. *Epilepsy and the functional anatomy of the human brain*. Boston: Little, Brown and Company, 1954. p. 193–4.
- Pijn JP, Van Neerven J, Noest A, Lopes da Silva FH. Chaos or noise in EEG signals; dependence on state and brain site. *Electroencephalogr Clin Neurophysiol* 1991; 79: 371–81.
- Salami M, Itami C, Tsumoto T, Kimura F. Change of conduction velocity by regional myelination yields constant latency irrespective of distance between thalamus and cortex. *Proc Natl Acad Sci USA* 2003; 100: 6174–9.
- Schiff SJ, Colella D, Jacyna GM, Hughes E, Creekmore JW, Marshall A, et al. Brain chirps: spectrographic signatures of epileptic seizures. *Clin Neurophysiol* 2000; 111: 953–8.
- Schiff SJ, Sauer T, Kumar R, Weinstein SL. Neuronal spatiotemporal pattern discrimination: the dynamical evolution of seizures. *Neuroimage* 2005; 28: 1043–55.
- Schindler K, Wiest R, Kollar M, Donati F. Using simulated neuronal cell models for detection of epileptic seizures in foramen ovale and scalp EEG. *Clin Neurophysiol* 2001; 112: 1006–17.
- Seba P. Random matrix analysis of human EEG data. *Phys Rev Lett* 2003; 91: 198104.
- Tian GF, Azmi H, Takano T, Xu Q, Peng W, Lin J, et al. An astrocytic basis of epilepsy. *Nat Med* 2005; 11: 973–81.
- Timofeev I, Steriade M. Neocortical seizures: initiation, development and cessation. *Neuroscience* 2004; 123: 299–336.
- Topolnik L, Steriade M, Timofeev I. Partial cortical deafferentation promotes development of paroxysmal activity. *Cereb Cortex* 2003; 13: 883–93.
- Wendling F, Bartolomei F, Bellanger JJ, Bourien J, Chauvel P. Epileptic fast intracerebral EEG activity: evidence for spatial decorrelation at seizure onset. *Brain* 2003; 126: 1449–59.
- Wendling F, Bellanger JJ, Badier JM, Coatrieux JL. Extraction of spatio-temporal signatures from depth EEG seizure signals based on objective matching in warped vectorial observations. *IEEE Trans Biomed Eng* 1996; 43: 990–1000.
- Wu L, Gotman J. Segmentation and classification of EEG during epileptic seizures. *Electroencephalogr Clin Neurophysiol* 1998; 106: 344–56.